

Cordycepin Ameliorates Dextran Sulfate Sodium-Induced Ulcerative Colitis in Mice by Inhibiting IL-6/IL-6R-Mediated p38 MAPK and NF-κB Activation Through Adenosine A_{2A} Receptor Stimulation

Yu Liao ¹, Weipeng Wei¹, Fuli Qin¹, Yusheng Ruan ¹, Ting He¹, Jiansong He ¹, Mingchao Wang², Taotao Liu ¹, Jiemei Chen¹

¹Department of Pharmacy, the First Affiliated Hospital of Guangxi Medical University, Nanning, People's Republic of China; ²Institute of Materia Medica, Chinese Academy of Medical Sciences and Peking Union Medical College, Beijing, People's Republic of China

Correspondence: Taotao Liu; Jiemei Chen, Email liutaotao@gxmu.edu.cn; chenjiemei@sr.gxmu.edu.cn

Background: Current ulcerative colitis (UC) therapies often cause adverse effects, and novel treatments are urgently needed. Cordycepin (COR), a bioactive compound from *Cordyceps militaris*, shows anti-inflammatory and intestinal protective potential, its precise role and mechanisms in UC remain unclear.

Purpose: This study aimed to elucidate the effects and underlying mechanisms of COR on UC.

Methods: Using dextran sulfate sodium (DSS)-induced acute colitis mice and DSS-damaged human colonic epithelial cells as models, we evaluated and analyzed the effects and mechanisms of COR on UC by combining molecular docking, molecular dynamics simulations, in vivo/in vitro interventions with selective pharmacological antagonists, transcriptome sequencing and Western blotting verification.

Results: In vitro experiments confirmed that COR exhibits protective effects on DSS-damaged colonic epithelial cells. Mechanistic studies revealed that COR elevates intracellular cAMP levels, and the selective adenosine A_{2A} receptor (A_{2A}AR) antagonist SCH58261 can block the protective effect of COR. Molecular docking and dynamics simulation analyses also demonstrated an interaction between COR and A_{2A}AR at the molecular level. In vivo experiments further verified that oral administration of COR (5 mg/kg, 10 mg/kg) significantly ameliorated DSS-induced colitis in mice, manifested by reduced disease activity index, attenuated weight loss, improved colon shortening, decreased serum pro-inflammatory cytokines, alleviated colonic inflammation, and restored intestinal barrier function. Moreover, the therapeutic effect of COR on colitis could be blocked by SCH58261. Further investigations indicated that COR inhibits IL-6/IL-6R signaling in colonic tissues and suppresses phosphorylation-mediated activation of p38 MAPK and NF-κB p65 through A_{2A}AR activation.

Conclusion: COR ameliorates DSS-induced colitis by activating A_{2A}AR to upregulate cAMP levels, inhibiting IL-6/IL-6R-mediated p38 MAPK and NF-κB activation. This study confirms A_{2A}AR as a key therapeutic target, providing data support for the potential application of COR in UC treatment.

Keywords: ulcerative colitis, adenosine receptor A_{2A}, cordycepin, colonic inflammation, intestinal barrier function

Introduction

Ulcerative colitis (UC) is a chronic relapsing inflammatory bowel disease characterized by inflammation that spreads continuously from the rectum in a proximal direction.¹ Currently, the health burden imposed by UC is escalating, with increasing trends observed in both its incidence and prevalence.² Current therapeutic agents include aminosalicylates, corticosteroids, immunosuppressants, and biologics. While these medications can alleviate symptoms, their long-term use



carries significant risks of serious adverse effects, such as immunosuppression and heightened susceptibility to infections. Although emerging therapeutic targets—including sphingosine 1-phosphate receptor modulators, janus kinase inhibitors, anti-leukocyte integrins—and fecal microbiota transplantation show considerable promise, many remain in stages of clinical development.³ Consequently, the development of novel, effective, and well-tolerated UC therapeutics is an urgent priority.

Cordyceps militaris is a medicinal and edible fungus containing numerous bioactive compounds. Cordycepin (COR), as one of its main components, possesses significant pharmacological value and has been reported to exhibit anti-tumor, anti-inflammatory, antioxidant, anti-apoptotic, metabolic regulatory, and neuroprotective activities.^{4–6} In recent years, one study reported that COR may modulate the intestinal Th1/Th2 and Th17/Treg cell balance and alter gut microbiota composition, thereby ameliorating colitis in mice.⁷ Additionally, our previous research found that COR alleviates high-fat and high-sugar diet-induced intestinal inflammation and oxidative stress damage, reduces intestinal epithelial cell apoptosis and pyroptosis, and improves intestinal barrier dysfunction in mice.⁸ This suggests COR may have potential therapeutic effects on colitis, but its precise role and mechanism remain to be elucidated.

Structurally, as an adenosine analogue, COR likely shares potential cellular targets with adenosine. Studies have reported that COR interacts with specific adenosine receptor (AR) subtypes (A_1AR , $A_{2A}AR$, A_3AR) in various contexts, exerting neuroprotective, metabolic regulatory, and anti-tumor effects.^{9–12} Critically, compelling evidence indicates a significant role for AR in the regulation of colitis.¹³ For instance, activation of the $A_{2A}AR$ modulates inflammatory responses and stimulates epithelial repair in experimental colitis. Gut microbiota-derived purine metabolites like inosine exert protective effects against colitis by enhancing intestinal mucosal barrier function through activating the $A_{2A}AR$ /peroxisome proliferators-activated receptor γ pathway.¹⁴ These findings suggest the critical regulatory role of AR activity in the pathogenesis of colitis. However, whether COR can ameliorate intestinal injury by modulating AR has not yet been reported in studies.

Additionally, targeting the IL-6 signaling pathway has emerged as a clinically relevant strategy in UC, given its central role in promoting chronic inflammation. Clinical trials of IL-6 pathway inhibitors have demonstrated efficacy in ulcerative colitis patients, highlighting the translational potential of modulating this axis.¹⁵

Therefore, this study employed dextran sulfate sodium (DSS)-damaged colonic epithelial cells to demonstrate the protective effect of COR, and preliminarily discovered that COR's protection of colonic epithelial cells is based on its activation of $A_{2A}AR$ through cyclic adenosine monophosphate (cAMP) level detection, AR subtype antagonist interference, molecular docking, and dynamics simulation (MD). Subsequently, in vivo experiments involving monitoring body weight, diarrhea, and rectal hemorrhage, histopathological staining of colon tissues, and detection of serum and colonic inflammatory factors, intestinal permeability markers, and cAMP levels further confirmed that COR ameliorates DSS-induced colitis in mice. Moreover, the therapeutic effect of COR on colitis could be blocked by SCH. Finally, transcriptome sequencing and pathway expression validation revealed that the ameliorative effect of COR on colitis was based on its activation of $A_{2A}AR$, thereby inhibiting IL-6/IL-6R-mediated phosphorylation activation of p38 MAPK and NF- κ B. This will provide data support for the application of COR in UC.

Materials and Methods

Materials and Reagents

Cordycepin (COR, CAS No. 73–03-0, Cat. No. C805132, 98% purity) was purchased from Shanghai Macklin Biochemical Technology Co., Ltd. (China); Dextran Sodium Sulfate (DSS, 60316ES60) was provided by Yeasen Biotechnology Co., Ltd. (Shanghai, China); Sulfasalazine (SASP, S129986) was obtained from Shanghai Aladdin Biochemical Technology Co., Ltd. (China); SCH58261 (HY-19533) and DPCPX (HY-100937) were supplied by MedChemExpress (MCE, Monmouth Junction, NJ, USA); BisBenzimide H 33342 (Hoechst 33342, C0030), and Propidium Iodide (PI, C0080) were purchased from Beijing Solarbio Science & Technology Co., Ltd. Proteintech Co., Ltd. (Wuhan, China), supplied the antibody against Zonula Occludens-1 (ZO-1, 21,773-1-AP), Occludin Polyclonal antibody (27260-1-AP), Adenosine A_1 receptor Polyclonal antibody (A_1AR , 20332-1-AP), the antibody against β -actin (20536-1-AP), CD126/IL-6R alpha Polyclonal antibody (23457-1-AP), Horseradish peroxidase (HRP)-conjugated goat

anti-rabbit secondary antibody (SA00001-2), and HRP-conjugated goat anti-mouse secondary antibody (SA00001-1). Adenosine A_{2A} receptor Antibody (A_{2A}AR, sc-32261) was purchased from Santa Cruz Biotechnology (USA). Antibodies against NF-κB p65 (8242T) and Phospho-NF-κB p65 (3033T) were obtained from Cell Signaling Technology (CST, USA). Antibodies against Phospho-p38 (R014105), Anti-p38 Rabbit mAb (R013794), Anti-STAT3 Rabbit pAb (P012881) and Anti-Phospho-STAT3 Rabbit mAb (R015031) were purchased from Epizyme (Shanghai, China). TNF-α (E-EL-H0109), IL-1β (E-EL-H0109), and IL-6 (E-EL-H6156) ELISA kits were purchased from Elabscience (Wuhan, China). The ECL detecting reagent (SQ201) was purchased from Shanghai Epizyme Biomedical Technology Co., Ltd. (China).

Cell Culture

The human intestinal epithelial cell line NCM460 (BNCC339288, China) was cultured in RPMI 1640 medium (C11875500BT, Gibco, US) supplemented with 10% fetal bovine serum (FBS, SR-01021, Oricell, Guangzhou, China), 50 U/mL penicillin, and 50 U/mL streptomycin. Cells were maintained at 37 °C in a humidified atmosphere containing 5% CO₂. The effects of different concentrations of COR and DSS on NCM460 cell viability were assayed using the CCK-8 kit (C6005M, UElandy, Suzhou, China).

Lactate Dehydrogenase (LDH) Activity Assay

After serum starvation with 2% FBS for 6 h, NCM460 cells were treated with 2% DSS, and / or 1 μmol/L COR, 10 μmol/L COR, 5 μmol/L SCH, or 5 μmol/L DPCPX for 24 h. The cell culture supernatant was collected, and the LDH activity in the supernatant was measured according to the instructions of the LDH assay kit (E-BC-K766-M, Elabscience, Wuhan, China).

Inflammatory Cytokine Assay

Following the aforementioned intervention, cell culture supernatants were collected. Levels of the pro-inflammatory cytokines TNF-α, IL-1β, and IL-6 were quantified according to the instructions of ELISA kits.

cAMP Quantification

cAMP levels in serum and cell lysates were measured using a competitive ELISA kit (E-EL-0056, Elabscience). The serum was pretreated by centrifugation at 1000×g. After treated according to the aforementioned method, 10⁶ NCM460 cells were collected from each group, and cell lysis was performed through freeze-thaw cycles. Detection was carried out according to the protocol instructions. The concentration was calculated based on OD450 readings against the standard curve.

Cell Death Quantification

Following the aforementioned intervention, NCM460 cells without fixation were sequentially stained with Hoechst 33342 (10 μg/mL) and PI (15 μg/mL). Nuclear morphology was analyzed using laser confocal microscopy (Olympus, Wetzlar, Germany). Cells exhibiting PI⁺ staining with condensed/fragmented nuclei were defined as dead cells. Death rates were calculated from five random fields/sample across triplicates.

Molecular Docking

Download the 2D structural formula of COR from the PubChem database, import it into Chem3D software for energy minimization, and export it in mol2 format. Import the mol2-formatted COR structure into AutoDock software and export it as pdbqt format. Search for the ADORA2A protein in the Uniprot database, with the species set as human, and select the X-ray or EM structure with the highest resolution to download as a PDB structure. Retain the protein while removing water molecules to serve as the protein structure. Import the optimized protein structure into AutoDockTools-1.5.7 software, neutralize charges, add hydrogen atoms, remove non-standard amino acids, and export it as pdbqt format. Select the ligand structure within the protein as the docking pocket, and perform molecular docking between the protein and small molecule using AutoDock Vina.

Molecular Dynamics (MD) Simulation

The complex was subjected to 100 ns MD simulation using Gromacs 2022. The protein was modeled with CHARMM 36¹⁶ force field parameters, while the ligand topology was constructed using GAFF2 force field parameters. Periodic boundary conditions were applied, and the protein-ligand complex was placed in a cubic box. The TIP3P water model was used to solvate the system, filling the box with water molecules to form a periodic boundary of 1.2 nm.¹⁷ Electrostatic interactions were treated using the Particle Mesh Ewald (PME) method and the Verlet algorithm, respectively. Subsequently, equilibration was performed under isothermal-isochoric (NVT) and isothermal-isobaric (NPT) ensembles for 50,000 steps each, with a coupling constant of 0.1 ps and a duration of 100 ps simulation. Both van der Waals and Coulomb interactions were calculated using a cutoff of 1.0 nm. Finally, the system underwent MD simulation under constant temperature (310 K) and pressure (1 bar) using Gromacs 2022 for a total duration of 100 ns.

Animal Experiments

Male C57BL/6J mice (8 weeks old; body weight: 20–22 g) were purchased from SPF (Beijing) Biotechnology Co., Ltd. (License No.: SYXK (Jing) 2024–0001). All experimental procedures strictly adhered to the National Research Council *Guide for the Care and Use of Laboratory Animals* and were approved by the Animal Care and Ethics Committee of Guangxi Medical University (Approval No.: 2025-D0342).

Mice were housed in a specific pathogen-free barrier facility (temperature: $22 \pm 1^\circ\text{C}$; relative humidity: $50 \pm 5\%$; 12-h light/dark cycle) with ad libitum access to standard rodent chow and drinking water. After a one-week acclimatization period, the mice were randomly divided into six groups (n=8 per group): (1) the Control group, (2) the DSS group, (3) the DSS + SASP group, (4) the DSS + COR-L group, (5) the DSS + COR-H group and (6) the DSS + SCH + COR-H group. Except for the control group, which consumed distilled water throughout the study, mice in all other groups were given a 5% (w/v) dextran sulfate sodium (DSS) solution dissolved in distilled water for 7 consecutive days (days 1–7) to induce acute colitis, followed by switching to normal distilled water alone on days 8–10. PStarting from the induction of DSS, the control and DSS groups received daily oral gavage of saline, while the DSS + COR-L and DSS + COR-H groups received daily oral gavage of 5 mg/kg or 10 mg/kg COR (dissolved in distilled water), respectively. Mice in the DSS + SCH + COR-H group were intraperitoneally injected with 2 mg/kg SCH58261 (SCH, dissolved in sterile corn oil) and administered 10 mg/kg COR by gavage daily. Mice in the DSS + SASP group were gavaged with 250 mg/kg sulfasalazine (SASP, dissolved in a 0.5% sodium carboxymethylcellulose solution) daily.

Body weight, food intake, stool consistency, and fecal blood were monitored and recorded daily. Disease activity index (DAI) was calculated according to established criteria and the DAI scores criteria were shown in [Table S1](#).¹⁸ On day 10, mice were fasted for 12 h and then anesthetized using isoflurane. Whole blood was collected via retro-orbital venous plexus puncture and was centrifuged at 4°C , $2000 \times g$ for 10 min after standing at room temperature to obtain serum. Serum samples were aliquoted and stored in a -80°C freezer for subsequent analysis. Following anesthesia, mice were euthanized, and the entire colon was immediately harvested and photographed for macroscopic assessment. The colon was then divided into two segments: one segment was fixed in 4% paraformaldehyde for histological analysis, and the other segment was rapidly frozen in liquid nitrogen.

Serum Cytokine Measurements

Serum cytokines were detected using BioLegend's LEGENDplex™ Mouse Inflammation Panel (740446, BioLegend) according to the manufacturer's protocol. Samples were analyzed on a Beckman CytoFlex flow cytometer. Standard curves were generated using kit-provided lyophilized standards, and raw data (.fcs files) were processed through BioLegend's cloud-based LEGENDplex™ Data Analysis Suite for automated analyte quantification.

Serum C-Reactive Protein (CRP) Quantification

Serum CRP levels were measured using a mouse-specific sandwich ELISA kit (E-EL-M0053, Elabscience). Serum samples were diluted, incubated, and analyzed according to the manufacturer's protocol. Absorbance was measured at

450 nm using an Epoch microplate reader (BioTek Instruments, Inc). Concentration values were calculated based on the standard curve.

Assessment of Intestinal Permeability Biomarkers

Serum diamine oxidase (DAO) levels were quantitatively measured using an ELISA kit (E-EL-M0412, Elabscience, Wuhan, China), while serum D-lactate concentrations were determined using a colorimetric assay kit (S0204S, Beyotime, Shanghai, China). Both assays were performed according to the manufacturer's protocols, with concentration values calculated based on standard curves.

Hematoxylin and Eosin (H&E) Staining

The colon tissue fragments were fixed with 4% paraformaldehyde, then embedded in paraffin and sectioned. (4 μ m). The sections were processed according to standard protocols using H&E staining reagents (G1076, Servicebio). Whole-slide digital images were acquired using an AMX CSS V1 scanner, with five randomly selected high-power fields analyzed per section. The histopathological scoring criteria were detailed in [Table S2](#).¹⁹

Alcian Blue / Periodic Acid-Schiff (AB/PAS) Staining

The colonic paraffin sections were stained with AB/PAS kit (G1049, Servicebio) for mucin / goblet cell assessment. Five non-consecutive fields per section were analyzed to evaluate goblet cell numbers. Goblet cell density was quantitated using ImageJ software (NIH, Bethesda, MD, USA).

TUNEL Apoptosis Assay

The colonic paraffin sections underwent standard dewaxing and rehydration procedures. After completing the standard pretreatment process, the sections were co-incubated with terminal deoxynucleotidyl transferase-mediated dUTP Nick-end labeling (TUNEL) reaction mixture (G1502, Servicebio). Nuclei were counterstained with DAPI (G1012, Servicebio) and observed under a fluorescence microscopy (Nikon Eclipse C1). Five random fields of view were selected for each section, and apoptotic cells were quantitatively analyzed using ImageJ software.

Quantitative Transcriptomics Analysis

Total RNA was extracted from colon tissues using the MJZol Total RNA Extraction Kit (Majorbio, Shanghai, China). RNA purity and integrity were assessed using NanoDrop 2000 (Thermo Fisher Scientific) and Agilent 5300 Bioanalyzer, respectively. High-quality RNA (OD_{260/280} = 1.8–2.2, RQN \geq 6.5) was used for library preparation. Poly(A)⁺ mRNA was enriched using Oligo(dT) magnetic beads, fragmented chemically, and used to construct strand-specific cDNA libraries following the Illumina[®] Stranded mRNA Prep protocol. Libraries were sequenced on the DNBSEQ-T7 platform (BGI, China) using PE150 chemistry. Raw sequencing reads were quality-controlled and filtered using fastp. Processed reads were aligned to the mouse reference genome using HISAT2. Transcript abundance was quantified as transcripts per million (TPM) using RSEM. Differential expression analysis between experimental groups was performed using DESeq2 with significance thresholds of $|\log_2 FC| \geq 1$ and false discovery rate (FDR) < 0.05. The protein-protein interaction (PPI) network was extracted from the STRING database (<https://string-db.org/cgi/input.pl>) with a minimum interaction score set at the highest confidence level of 0.4. Parameters such as degree, betweenness, and closeness were acquired using the Centiscape2.2 plug-in. The resultant PPI network was then visualized through Cytoscape 3.8.2 software. Reactome enrichment analysis was conducted using Goatool and SciPy.

Western Blot Analysis

Tissue and cell protein samples were separated by SDS-PAGE and transferred to PVDF membranes. After blocking in 5% non-fat milk/TBST, membranes were probed overnight at 4°C with primary antibodies: anti-ZO-1 (1:5000), anti-Occludin (1:5000), anti-A₁AR (1:1000), anti-A_{2A}AR (1:1000), anti-p65 (1:1000), anti-P-p65 (1:1000), anti-p38 (1:1000), anti-P-p38 (1:1000), anti-IL-6R (1:1000), anti-STAT3 (1:500), anti-P-STAT3 (1:1000) and anti- β -actin (1:10,000). Following secondary HRP-antibody incubation (1:5000, species-matched), protein bands were detected by

ECL chemiluminescence (Tanon 4600). Target protein expression was quantified via ImageJ densitometry normalized to β -actin.

Statistical Analysis

All quantitative data are presented as mean \pm standard error of mean (SEM) and were statistically analyzed using GraphPad Prism software (Version 9.5.0, San Diego, CA, USA). Inter-group comparisons between two independent samples were performed using two-tailed unpaired Student's *t*-test, while multi-group comparisons were assessed by one-way ANOVA. For non-normally distributed variables, inter-group statistical significance was evaluated via Kruskal–Wallis test. A value of $P < 0.05$ was considered statistically significant.

Results

Cordycepin Alleviates DSS-Induced Damage to Intestinal Epithelial Cells

Intestinal epithelial cells, serving as the body's first line of defense against pathogenic microorganisms, constitute a crucial component of the intestinal barrier. Therefore, we employed DSS to treat NCM460 cells *in vitro* to simulate colitis for preliminary evaluation of the protective effects of COR. CCK8 assays indicated NCM460 cell viability declined with increased DSS exposure, with higher concentrations causing more significant decreases (Figure 1A). Thus, 2% DSS was chosen for further experiments. COR did not significantly affect cell viability at concentrations up to 10 $\mu\text{mol/L}$ (Figure 1B), leading to the selection of 1 $\mu\text{mol/L}$ and 10 $\mu\text{mol/L}$ as treatment concentrations.

Experimental results demonstrated that 2% DSS treatment for 24 h induced marked damage to NCM460 cells, evidenced by increased release of the cell damage marker LDH and elevated levels of inflammatory cytokines IL-1 β , IL-6, and TNF- α in the supernatant (Figure 1C–F). PI staining further confirmed a significant rise in NCM460 cell death (Figure 1G). Additionally, 2% DSS notably downregulated ZO-1 protein expression (Figure 1H). In contrast, both 1 $\mu\text{mol/L}$ and 10 $\mu\text{mol/L}$ COR significantly reduced the 2% DSS-induced release of LDH, IL-1 β , IL-6, and TNF- α , while markedly suppressing NCM460 cell death (Figure 1C–G). Furthermore, 10 $\mu\text{mol/L}$ COR distinctly upregulated ZO-1 protein expression (Figure 1H). These findings collectively indicated that COR possesses a protective effect on intestinal epithelial cells.

Cordycepin Inhibits DSS-Induced Damage to Intestinal Epithelial Cells by Activating Adenosine Receptor A_{2A}

COR shares a highly similar chemical structure with adenosine, suggesting it may exert adenosine-like effects by activating AR. There are four known subtypes of AR: A₁AR, A_{2A}AR, A_{2B}AR, and A₃AR. To determine whether COR improves colitis by activating AR and which subtype is involved, we measured cAMP levels in NCM460 cells. The results showed that 2% DSS significantly downregulated intracellular cAMP levels in NCM460 cells, while 1 $\mu\text{mol/L}$ and 10 $\mu\text{mol/L}$ COR significantly upregulated cAMP levels (Figure 2A). These findings suggest that COR likely activates A_{2A}AR or A_{2B}AR. Existing literature predominantly indicates that activating the A_{2A}AR ameliorates colitis,^{14,20–22} whereas some studies report that A_{2B}AR activation may exacerbate colitis.^{23–25} Therefore, we hypothesized that COR protects intestinal epithelial cells primarily by activating the A_{2A}AR.

To test this, we used the selective competitive A_{2A}AR antagonist SCH to interfere with NCM460 cells for preliminary validation. The results revealed that SCH further reduced the DSS-induced decline in cAMP levels and blocked the cAMP-elevating effect of 10 $\mu\text{mol/L}$ COR (Figure 2B). Correspondingly, SCH abolished COR's inhibitory effects on DSS-induced LDH, IL-1 β , IL-6, and TNF- α release in NCM460 cells (Figure 2C–F). Moreover, SCH also blocked COR's ability to reduce DSS-induced cell death and upregulate ZO-1 protein levels (Figure 2G and H). However, the adenosine A₁ receptor antagonist DPCPX did not inhibit COR's cAMP-enhancing effect (Figure 2B). Accordingly, under DPCPX interference, COR still significantly reduced DSS-induced LDH, IL-1 β , and IL-6 release, mitigated cell death, and upregulated ZO-1 protein levels (Figure 2C–H). Additionally, neither DSS nor COR (1 $\mu\text{mol/L}$ and 10 $\mu\text{mol/L}$) altered the protein expression of A_{2A}AR or A₁AR (Figure 2I and J). These results demonstrated that COR may alleviate

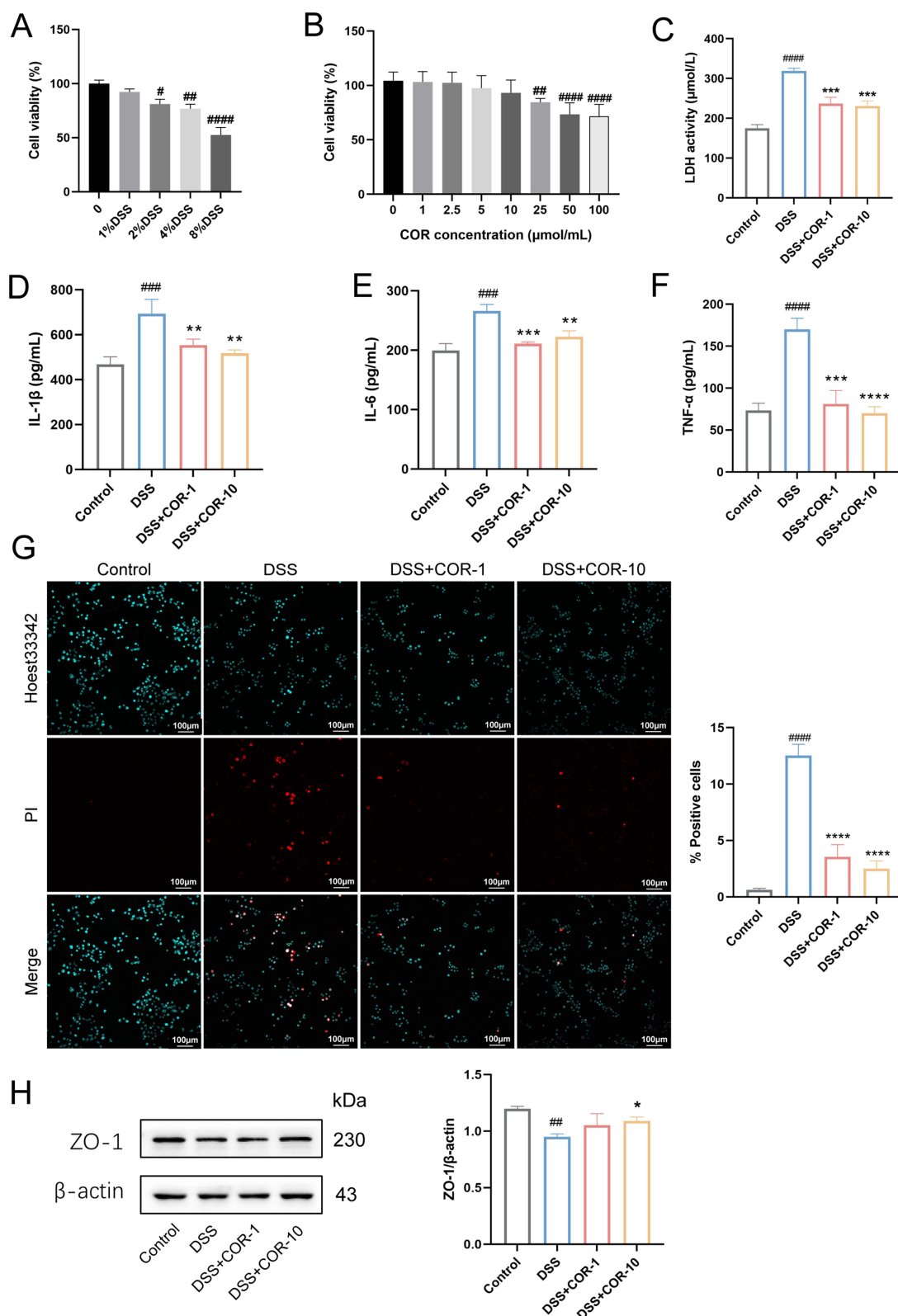


Figure 1 Cordycepin mitigates 2% DSS-induced damage in NCM460 cells. **(A)** Effects of different concentrations of DSS on the viability of NCM460 cells. **(B)** Effects of different concentrations of cordycepin (COR) on the viability of NCM460 cells. NCM460 cells were treated with 2% DSS and / or 1 $\mu\text{mol/L}$ (COR-1), 10 $\mu\text{mol/L}$ (COR-10) COR for 24 h, the release levels of **(C)** LDH, **(D)** IL-1 β , **(E)** IL-6, and **(F)** TNF- α in the supernatant were measured by using Elisa. **(G)** Representative images of PI staining and the percentage of PI-positive cells, scar bar = 100 μm . **(H)** The protein expression of ZO-1 in NCM460 cells was determined by using Western blotting assay. The results were representative of three independent experiments and expressed as mean \pm SEM. Data were compared using two-tailed Student's t tests. # $P < 0.05$, ## $P < 0.01$, ### $P < 0.001$ and #### $P < 0.0001$ vs. control group; * $P < 0.05$, ** $P < 0.01$, *** $P < 0.001$ and **** $P < 0.0001$ vs. the 2% DSS group.

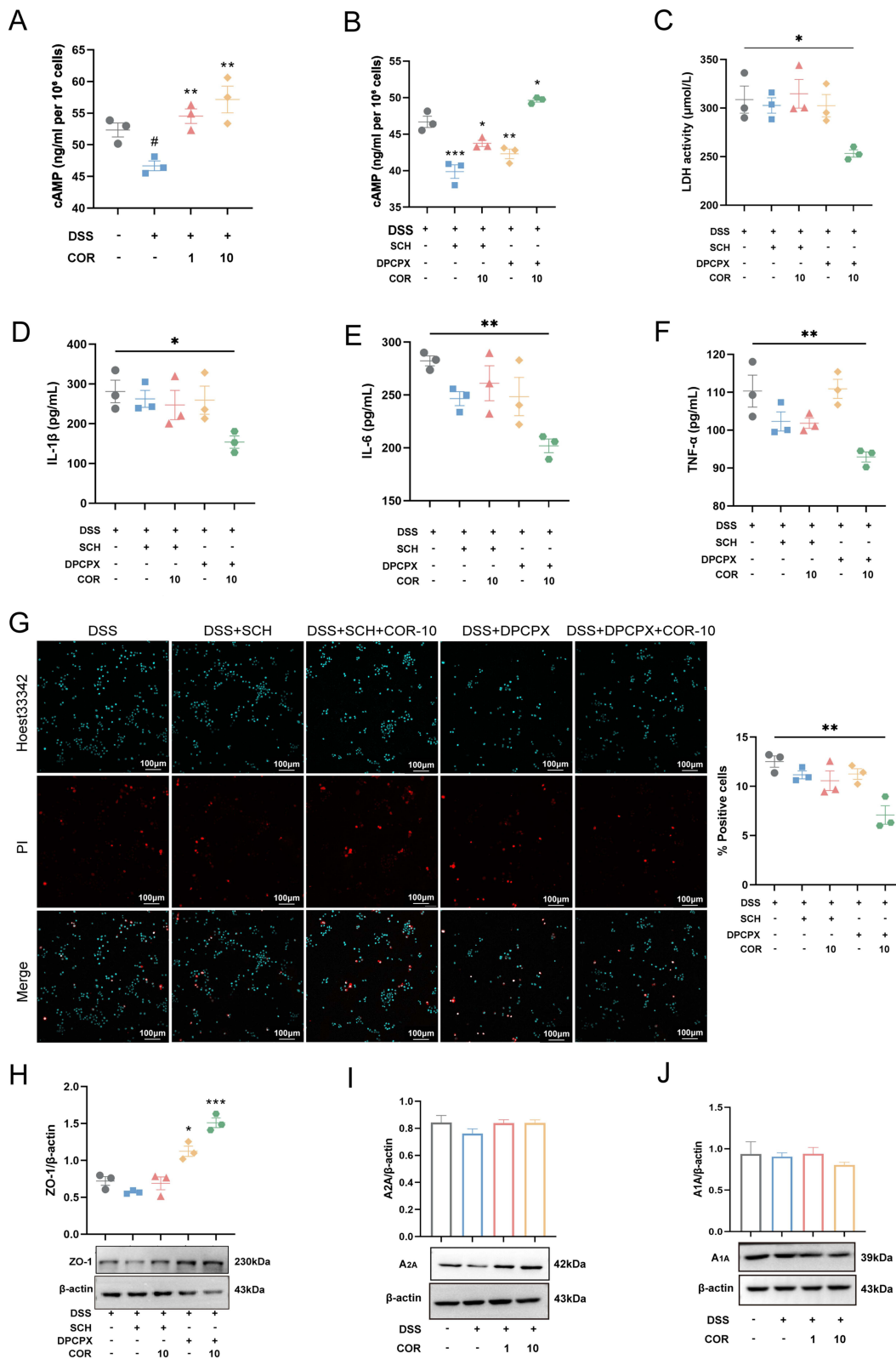


Figure 2 Cordycepin abates DSS-induced damage in NCM460 cells by activating adenosine receptor A_{2A} . **(A)** The cAMP levels in NCM460 cells under treatment with 2% DSS and/or 1 μ mol/L and 10 μ mol/L COR. **(B)** The cAMP levels in NCM460 cells under treatment with 2% DSS, 10 μ mol/L COR, 5 μ mol/L SCH58261 (SCH), and / or 5 μ mol/L DPCPX for 24 h. The release levels of **(C)** LDH, **(D)** IL-1 β , **(E)** IL-6, and **(F)** TNF- α were measured by using Elisa. **(G)** Representative images of PI staining and the percentage of PI-positive cells, scar bar = 100 μ m. **(H-J)** The protein expression of ZO-1, A_{2A} AR and A_1 AR in NCM460 cells was determined by using Western blotting assay. The results were representative of three independent experiments and expressed as mean \pm SEM. Data were compared using two-tailed Student's t tests. vs. control group; #P < 0.05, vs. control group; *P < 0.05, **P < 0.01 and ***P < 0.001 vs. the 2% DSS group.

Abbreviations: COR, cordycepin; SCH, SCH58261; DPCPX, 1,3-Dipropyl-8-cyclopentylxanthine; A_{2A} AR, adenosine receptor A_{2A} ; A_1 AR, adenosine receptor A_1 .

DSS-induced damage to intestinal epithelial cells by activating the A_{2A}AR rather than upregulation expression of A_{2A}AR.

Molecular Docking and Molecular Dynamics Simulation of Adenosine Receptor A_{2A}-Cordycepin

To elucidate whether COR interacts with the A_{2A}AR, we performed molecular docking and dynamics simulations between COR and the A_{2A}AR. As shown in **Figure 3A**, the docking score of COR with the A_{2A}AR protein (PDB ID: 5nm4) was -7.0 kcal/mol. COR formed a hydrogen bond with ALA68 of the A_{2A}AR protein at a distance of 2.82 Å, while also establishing hydrophobic interactions with PHE-71, ALA-72, ILE-89, ALA-90, VAL-93, PHE-177, MET-186, LEU-354, ASN-358, and ILE-379.

During the 100 ns MD simulation, the A_{2A}AR-COR complex system reached equilibrium after 50 ns, ultimately fluctuating around 3.8 Å, indicating structural stability (**Figure 3B**). The number of hydrogen bonds formed by the complex during the MD simulation fluctuated continuously between 0 and 5 (**Figure 3C**). Furthermore, the root mean square fluctuation (RMSF) values of the A_{2A}AR-COR complex were remaining below 8 Å (**Figure 3D**). Solvent-accessible surface area (SASA) analysis revealed slight fluctuations during the motion of the complex, which gradually stabilized (**Figure 3E**), suggesting that the binding of the small molecule affects the binding microenvironment and leads to certain changes in SASA. The radius of gyration (Rg) of the A_{2A}AR-COR complex exhibited stable fluctuations during motion (**Figure 3F**), demonstrating that the complex possesses a stable and compact structure. These results indicate that A_{2A}AR-COR can form stable interactions at the molecular level.

Pharmacological Inhibition of Adenosine Receptor A_{2A} Blocks Cordycepin's Ameliorative Effects on DSS-Induced Acute Colitis Symptoms in Mice

On this basis, we employed DSS to induce acute colitis in mice to verify the ameliorative effect of cordycepin on colitis and investigate the role of A_{2A}AR in this process. DSS-induced colitis is a model that replicates human UC symptoms, such as weight loss, diarrhea, and rectal bleeding. Mice were exposed to DSS for 7 days and then given normal water for 3 days. COR, SCH and SASP were administered daily for 10 days. The detailed experimental protocol is illustrated in **Figure 4A**. The results showed that DSS mice had significant weight loss, elevated DAI scores, shorter colon lengths compared to controls (**Figure 4B–D**). Serum levels of pro-inflammatory cytokines like TNF- α , IL-1 β , IL-6, IFN- γ , and CRP were also elevated (**Figure 4E–I**). Histological analysis revealed colitis-related changes in the DSS group, including muscle fiber separation, submucosal edema, inflammatory cell infiltration, and crypt structure loss (**Figure 4J and K**). These findings collectively indicate the successful establishment of an acute colitis model in mice induced by DSS.

Compared with the DSS model group, both COR (COR-L and COR-H) and the SASP administration groups significantly reduced body weight loss, decreased DAI scores, and mitigated colon length shortening in colitis mice (**Figure 4B–D**). Additionally, COR (COR-L and COR-H) and SASP administration also lowered the serum levels of TNF- α , IL-1 β , IL-6, IFN- γ , and CRP, and mitigated colonic tissue damage, reducing histopathological scores (**Figure 4E–K**). These results demonstrated that COR (5 mg/kg and 10 mg/kg) exhibits comparable efficacy to 250 mg/kg SASP in alleviating DSS-induced colitis.

Moreover, as expected, the results showed that under SCH intervention, nor could COR inhibit weight loss, increased DAI scores, or colon shortening in colitis mice (**Figure 4B–D**). Additionally, SCH also blocked COR's effects of reducing serum levels of TNF- α , IL-1 β , IL-6, IFN- γ , and CRP, as well as mitigating muscularis propria separation, submucosal edema, inflammatory cell infiltration, and villous damage in colon tissues, thereby lowering histopathological scores (**Figure 4E–K**). These findings indicate that COR's effects were inhibited by SCH, demonstrating that COR improves colitis symptoms by activating the A_{2A}AR.

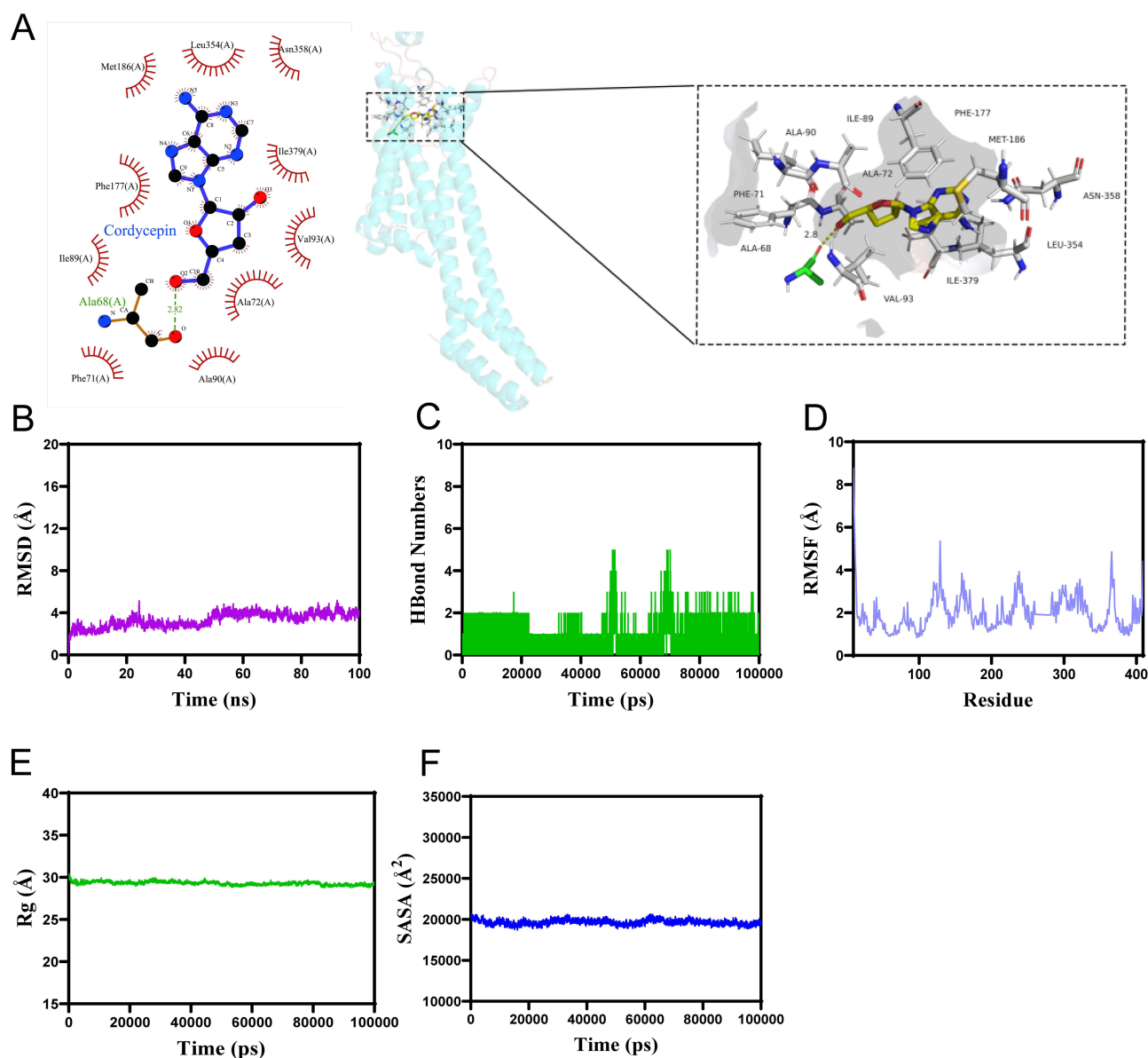


Figure 3 The results of molecular docking and molecular dynamics simulation of adenosine receptor A_{2A} -cordycepin. **(A)** 2D (left) and 3D (right) molecular docking diagrams of A_{2A} AR-COR. The PDB ID of the A_{2A} AR protein is 5nm4. The yellow stick represents the structure of COR, and the cartoon depicts the protein structure. The green sticks indicate amino acid residues within 4 Å that form hydrogen bonds with COR. Yellow dashed lines represent hydrogen bonds, with adjacent numbers denoting the distance between COR and the hydrogen-bonded amino acids. White sticks represent amino acids involved in hydrophobic interactions with COR. **(B)** The Root Mean Square Deviation (RMSD). **(C)** The number of hydrogen bonds of the complex. **(D)** The Root Mean Square Fluctuation (RMSF) values for the complex. **(E)** The Radius of Gyration (Rg) values of the complex. **(F)** Solvent Accessible Surface Area (SASA) of the complex.

Abbreviations: COR, cordycepin; A_{2A} AR, adenosine receptor A_{2A} .

Pharmacological Inhibition of Adenosine Receptor A_{2A} Blocks Cordycepin's Amelioration of Intestinal Inflammation and Gut Barrier Function in Colitis Mice

To assess COR's protective impact on colitis, cytokine levels in colon tissues were measured. COR at effective doses (5 mg/kg and 10 mg/kg) significantly lowered the levels of colonic IL-1 β , IL-6, and TNF- α in colitis mice (Figure 5A–C), indicating COR mitigates DSS-induced colonic inflammation. AB-PAS staining results revealed that DSS reduced mucin content and goblet cell numbers in colons, whereas COR administration (COR-L and COR-H) increased both mucin content and goblet cell numbers in mice (Figure 5D and E). Additionally, TUNEL staining results showed a significant increase in TUNEL-positive cells in the DSS model group, which was markedly reduced in the COR-treated groups (Figure 5F and G), demonstrating that COR significantly decreases DSS-induced apoptosis. Furthermore, COR treatment

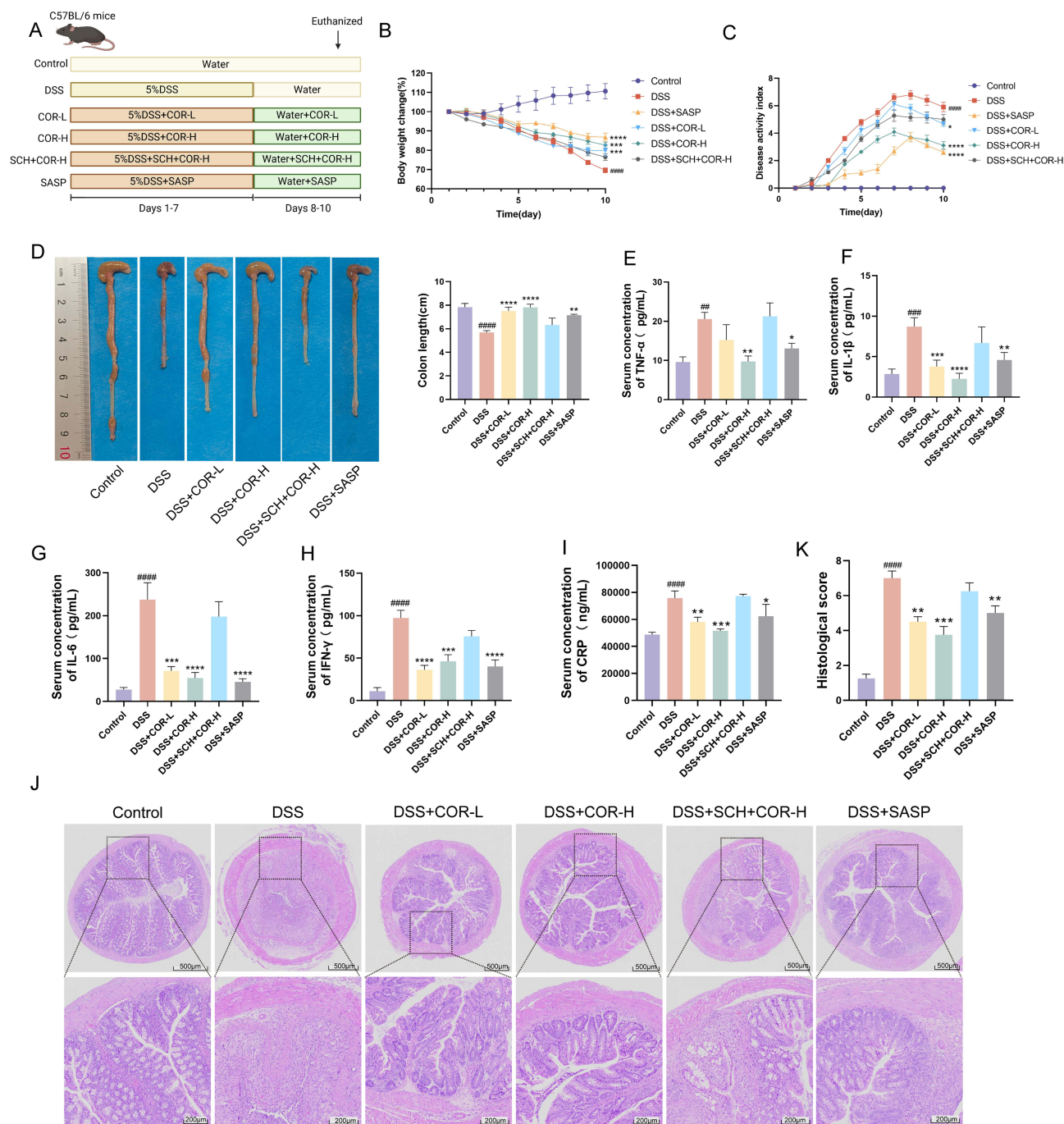


Figure 4 SCH58261 blocks cordycepin's ameliorative effects on DSS-induced acute colitis symptoms in mice. **(A)** Animal experimental flowchart. **(B)** The body weight change. **(C)** The disease activity index (DAI). **(D)** The colon length. **(E-I)** Serum level of TNF- α , IL-1 β , IL-6, IFN- γ and CRP. **(J)** The histopathological damage of colons was detected by using H&E staining. **(K)** Histological score. Data were presented as the means \pm SEM of six-eight mice in each group and were compared using two-tailed Student's t tests. ##P < 0.01, ###P < 0.001 and ####P < 0.0001 vs. control group; *P < 0.05, **P < 0.01, ***P < 0.001 and ****P < 0.0001 vs. the DSS model (DSS) group. **Abbreviations:** COR, cordycepin; SASP, sulfasalazine.

also reversed the DSS-induced reduction in the expression of critical intestinal tight junction proteins ZO-1 and Occludin (Figure 5H). In the DSS model group, serum D-lactate (a marker of intestinal permeability) and DAO (a marker of intestinal injury) levels were significantly elevated, whereas these levels were notably reduced in the COR-treated groups (Figure 5I and J). Importantly, SCH intervention inhibited COR's effect on reducing the levels of inflammatory cytokines TNF- α , IL-1 β , and IL-6 (Figure 5A-C). AB-PAS staining results showed that blocking the A_{2A}AR also suppressed COR's

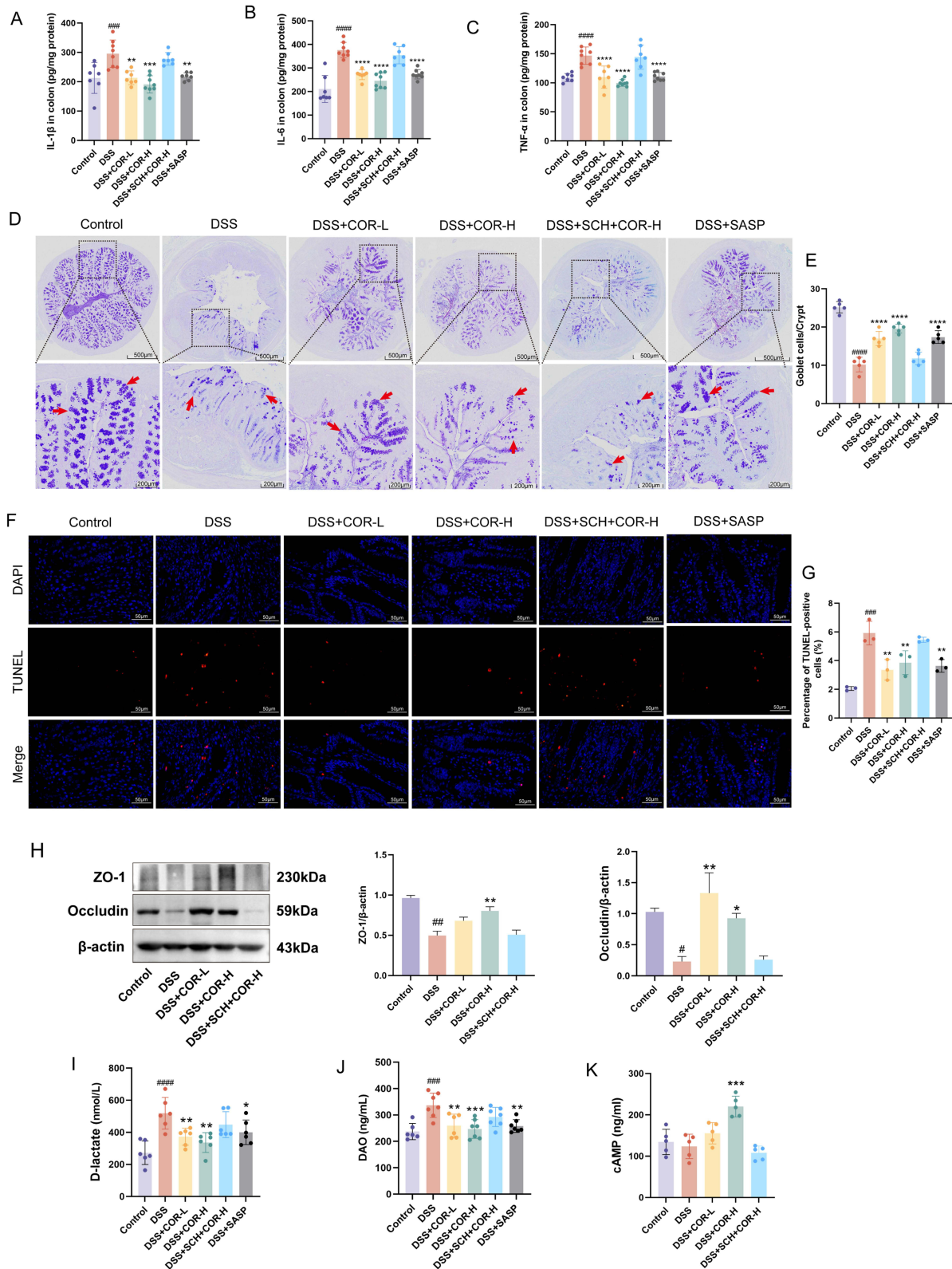


Figure 5 SCH58261 blocks cordycepin's amelioration of intestinal inflammation and gut barrier function in DSS-induced colitis mice. **(A–C)** Level of colonic IL-1 β , IL-6, and TNF- α among the Control, DSS, DSS+COR-L and DSS+COR-H group were detected by using Elisa. **(D)** Representative images of AB-PAS staining of colonic tissue. The arrow indicates the goblet cells. **(E)** Number of goblet cells in colonic tissue. **(F)** Representative images of TUNEL staining in colonic tissue, scale bar = 50 μ m. **(G)** Percentage of TUNEL-positive cells (%). **(H)** The protein expression of ZO-1 and Occludin in colons was determined by using Western blotting assay. **(I)** and **(J)** Serum level of D-lactate and diamine oxidase (DAO) were measured by using Elisa. **(K)** The serum cAMP levels among the control, DSS, DSS+COR-L, DSS+COR-H group and DSS+SCH+COR-H group. Data were presented as the means \pm SEM of six-eight mice in each group and were compared using two-tailed Student's *t* tests. **P* < 0.05, ***P* < 0.01, ****P* < 0.001 and *****P* < 0.0001 vs. control group; **P* < 0.05, ***P* < 0.01, ****P* < 0.001 and *****P* < 0.0001 vs. the DSS model (DSS) group.

Abbreviations: COR, cordycepin; SASP, sulfasalazine.

ability to increase colonic mucin content and goblet cell numbers (Figure 5D and E). Additionally, SCH blocked COR's effects on reducing apoptosis in colonic tissues (Figure 5F and G) and upregulating protein expression of ZO-1 and Occludin (Figure 5H). Furthermore, SCH also inhibited COR's downregulation of serum D-lactate and DAO levels (Figure 5I and J). Additionally, serum cAMP levels were significantly increased by 10 mg/kg COR administration in colitis mice. In contrast, cAMP levels could not be upregulated by COR under SCH intervention (Figure 5K). These results collectively indicated that COR markedly ameliorates DSS-induced intestinal inflammation and impairment of intestinal barrier function by activating the $A_{2A}AR$.

Transcriptome Data Suggests That Cordycepin Activates Adenosine Receptor A_{2A} to Exert Colitis-Alleviating Effects by Regulating the IL-6 Signaling Pathway

To further elucidate the downstream protective mechanisms of COR upon $A_{2A}AR$ activation, we conducted transcriptome sequencing analysis of colon tissues. First, principal component analysis revealed distinct clustering patterns among groups, with the DSS+COR-H group showing closer proximity to the control group, while the DSS+SCH+COR-H group aligned more closely with the DSS group (Figure 6A). Differentially expressed genes were screened using the criteria of $P_{adj} < 0.05$ and fold change (FC) ≥ 2 or $FC \leq 0.5$. The results identified 2544 differentially expressed genes in DSS vs. Control, comprising 1887 upregulated and 657 downregulated genes (Figure 6B). DSS+COR-H vs. DSS exhibited 172 differentially expressed genes, including 60 upregulated and 112 downregulated genes (Figure 6B). Notably, DSS+SCH+COR-H vs. DSS showed only one differentially expressed gene, even without setting an FC threshold (Figure 6B). These findings demonstrated at the transcriptional level that COR alters the colon transcriptome profile in DSS-induced colitis mice, shifting it toward the control group, whereas SCH abolishes COR's effect on the transcriptional profile.

The Venn diagram in Figure 6C illustrates the intersection of differentially expressed genes among the four groups. There are 130 overlapping genes between the DSS vs Control and DSS+COR-H vs DSS comparisons. Unsupervised hierarchical clustering analysis using these overlapping genes also revealed that the DSS+COR-H group samples clustered with the control group samples, whereas the DSS group and DSS+SCH+COR-H group samples clustered together (Figure 6D). Protein-protein interaction network analysis of these overlapping differentially expressed genes identified IL-6 as the central hub node (Figure 6E). IL-6 is known to play a critical role in the pathogenesis, progression, and treatment of ulcerative colitis. Therefore, we speculate that IL-6 may be a key gene involved in COR-mediated amelioration of colitis.

Subsequently, to elucidate the potential regulatory pathways underlying the protective effects of COR, we performed Reactome enrichment analysis. As shown in Figure 6F, the differentially expressed genes between the DSS vs Control groups were significantly enriched in pathways such as extracellular matrix organization, collagen formation, integrin cell surface interactions, Interleukin-6 family signaling, O-linked glycosylation, IL-6-type cytokine receptor ligand interactions, and interleukin-6 signaling. In contrast, the differentially expressed genes between the DSS+COR-H vs DSS groups were primarily enriched in pathways including synthesis of substrates in N-glycan biosynthesis, TRP channels, GABA receptor activation, ion channel transport, glycosphingolipid biosynthesis, O-linked glycosylation, and interleukin-6 signaling (Figure 6G). Notably, the IL-6 signaling pathway was significantly enriched in both DSS vs Control and DSS+COR-H vs DSS comparisons, suggesting that the IL-6 signaling pathway may be a key effector pathway regulated by COR.

Cordycepin Activation of Adenosine Receptor A_{2A} Inhibits IL-6/IL-6R-Mediated p38 MAPK and NF- κ B Phosphorylation Activation

To clarify whether COR regulates the IL-6 signaling pathway, we analyzed the expression of key proteins in the IL-6 signaling pathway in colon tissues, including IL-6R, STAT3, NF- κ B p65, and p38 MAPK. The results showed that compared with the control group, the DSS group exhibited significantly increased expression of IL-6R and ratios of NF- κ B P-p65/p65, and P-p38/p38 MAPK in mouse colon tissues, while the P-STAT3/STAT3 ratio also showed an upward trend (Figure 7A–M). Compared with DSS, the COR-H group demonstrated significantly reduced expression of IL-6R

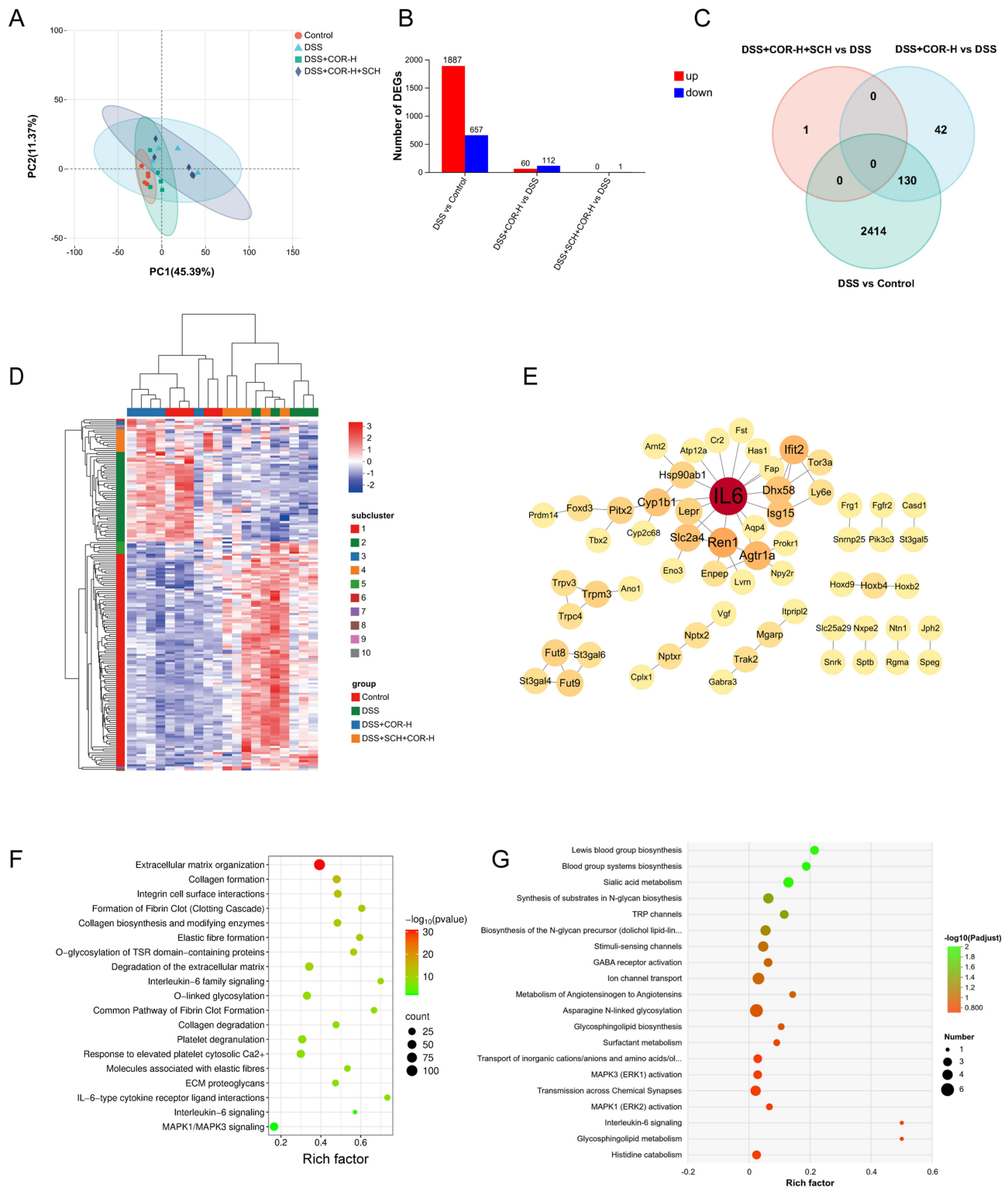


Figure 6 Cordycepin may exert its ameliorative effect on colitis by regulating the IL-6 signaling pathway. **(A)** Principal component analysis (PCA) plot of colon tissue transcriptomes. **(B)** Differential gene expression analysis: DSS vs Control (left), DSS+COR-H vs DSS (center), DSS+SCH+COR-H vs DSS (right). **(C)** Venn diagram of overlapping differentially expressed genes. **(D)** Hierarchical clustering heatmap of differentially expressed genes. **(E)** Protein-protein interaction network of intersecting differential genes. **(F)** Reactome enrichment analysis of the DSS group vs the control group. **(G)** Reactome enrichment analysis of the DSS+COR-H group vs the DSS group.

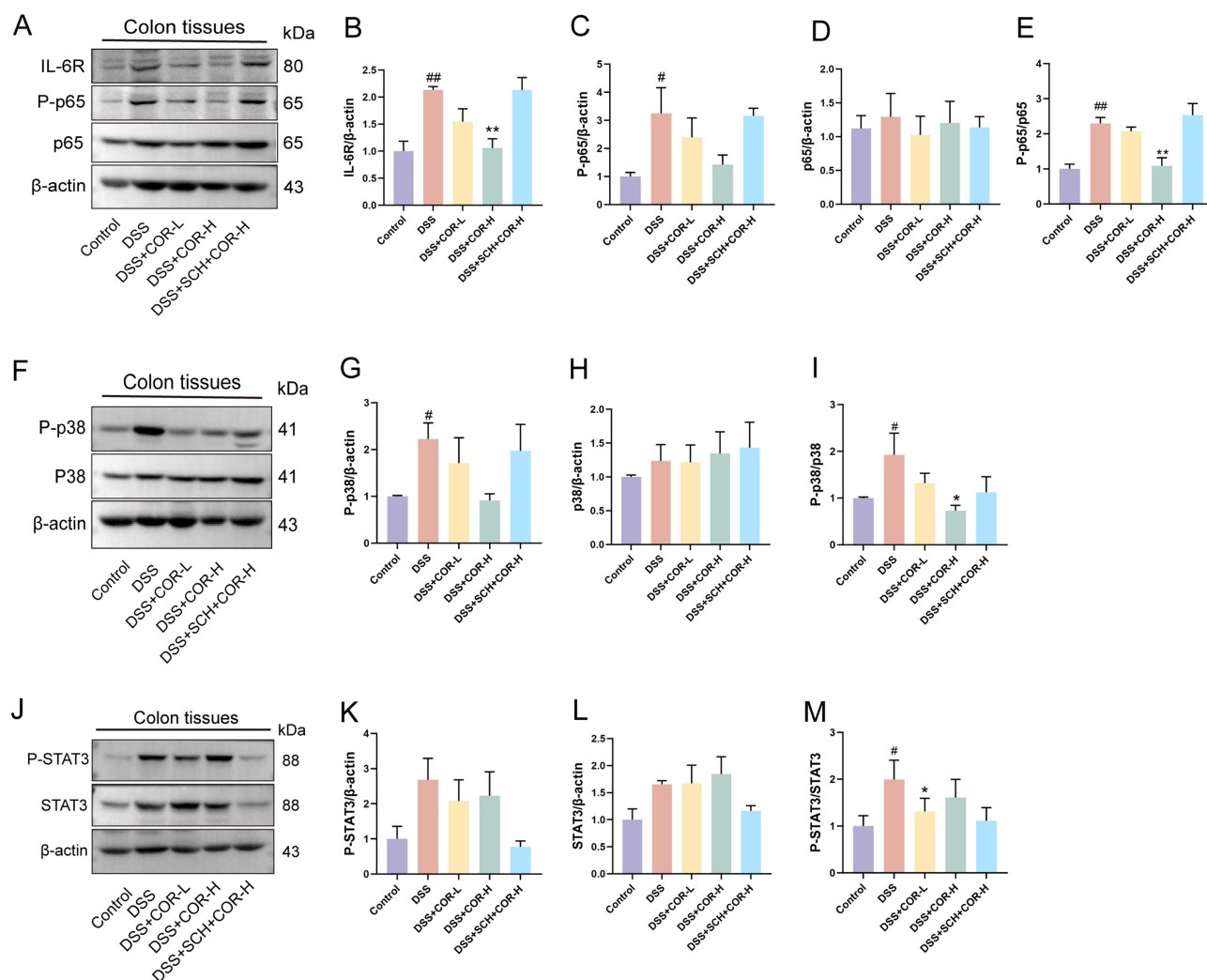


Figure 7 Cordycepin inhibits IL-6/IL-6R-mediated p38 MAPK and NF- κ B phosphorylation activation relying on activation of adenosine receptor A_{2A} . (**A–E**) Representative blot bands and relative expression levels for IL-6R, NF- κ B P-p65, NF- κ B p65, NF- κ B P-p65/p65, detected by Western blotting. (**F–I**) Representative blot bands and relative expression levels for P-p38 MAPK, p38 MAPK, P-p38/p38 MAPK. (**J–M**) Representative blot bands and relative expression levels for P-STAT3, STAT3, P-STAT3/STAT3. Data were presented as the means \pm SEM of three mice in each group and were compared using two-tailed Student's *t* tests. [#]*P* < 0.05, ^{##}*P* < 0.01 vs. control group; ^{*}*P* < 0.05, ^{**}*P* < 0.01 vs. the DSS model (DSS) group.

and ratios of NF- κ B P-p65/p65, and P-p38 /p38 MAPK, but no significant change in P-STAT3/STAT3 (Figure 7A–M). These results indicated that COR-H administration inhibited DSS-induced IL-6/IL-6R signaling and the phosphorylation activation of NF- κ B p65 and p38 MAPK in colon tissues. Additionally, it is noteworthy that co-administration of the A_{2A} AR antagonist SCH completely abolished the therapeutic effects of COR-H (Figure 7A–M). It is known that the phosphorylation activation of p38 MAPK and NF- κ B p65 are core mechanisms driving intestinal inflammatory responses. cAMP can also inhibit their activation, exerting beneficial effects such as anti-inflammatory and antioxidant stress.²⁶ These results suggested that the ameliorative effect of COR on DSS-induced colitis is attributed to its activation of A_{2A} AR, which inhibits IL-6/IL-6R-mediated phosphorylation activation of p38 MAPK and NF- κ B.

Discussion

In recent years, the incidence of UC has been continuously rising, making it particularly urgent to explore its prevention and treatment targets and develop novel therapeutic or adjuvant drugs with fewer toxic side effects. This study employed DSS-induced *in vitro* and *in vivo* colitis models to confirm the role of COR in protecting colonic epithelial cells, suppressing intestinal inflammation, and improving intestinal barrier function, thereby exerting a positive impact on

colitis amelioration. Mechanistic investigations revealed for the first time that COR, as an adenosine analog, activates $A_{2A}AR$ to upregulate intracellular cAMP levels, thereby achieving protective effects against DSS-induced damage in colonic epithelial cells. Molecular-level interaction analysis demonstrated that COR and $A_{2A}AR$ may form a stable binding through hydrogen bonds and hydrophobic interactions. In vivo experimental results also confirmed that the ameliorative effect of COR on DSS-induced murine colitis is dependent on $A_{2A}AR$ activation. Further studies found that COR-mediated $A_{2A}AR$ activation downregulates the expression of IL-6 and IL-6R in colonic tissues while suppressing the phosphorylation activation of critical pro-inflammatory regulators p38 MAPK and NF- κ B p65 (Figure 8). These findings suggested that as an $A_{2A}AR$ agonist, COR can block L-6/IL-6R signaling transduction, inhibit the activation of p38 MAPK and NF- κ B p65, and thus holds potential therapeutic value for ulcerative colitis.

COR has been reported to possess various pharmacological activities, including anti-obesity, anti-metabolic fatty liver, anti-tumor, anti-inflammatory, and antioxidant effects.^{6,8,9,27,28} Although one study reported that COR can regulate the balance of intestinal Th1/Th2 and Th17/Treg cells and the gut microbiota, thereby alleviating intestinal inflammation,⁷ our previous research also found that COR can mitigate intestinal damage in mice caused by a high-fat and high-sugar diet.⁸ However, the ameliorative effects and mechanisms of COR on UC remain incompletely understood. In this study, COR was shown to inhibit DSS-induced intestinal epithelial cell damage, reduce cell death, and upregulate ZO-1 protein expression, indicating a direct protective effect on intestinal epithelial cells. Furthermore, by using a DSS-induced acute UC mouse model, we demonstrated that COR alleviates colitis symptoms, reduces colonic inflammation levels, increases the number of goblet cells, inhibits apoptosis, upregulates ZO-1 protein expression, and decreases intestinal permeability markers such as serum D-lactate and intestinal damage markers like serum diamine oxidase levels, thereby improving colitis.

The chemical structure of COR is highly similar to adenosine, suggesting that it may exert biological effects primarily through AR via mechanisms analogous to those of adenosine. The AR family comprises four subtypes: A_1AR , $A_{2A}AR$,

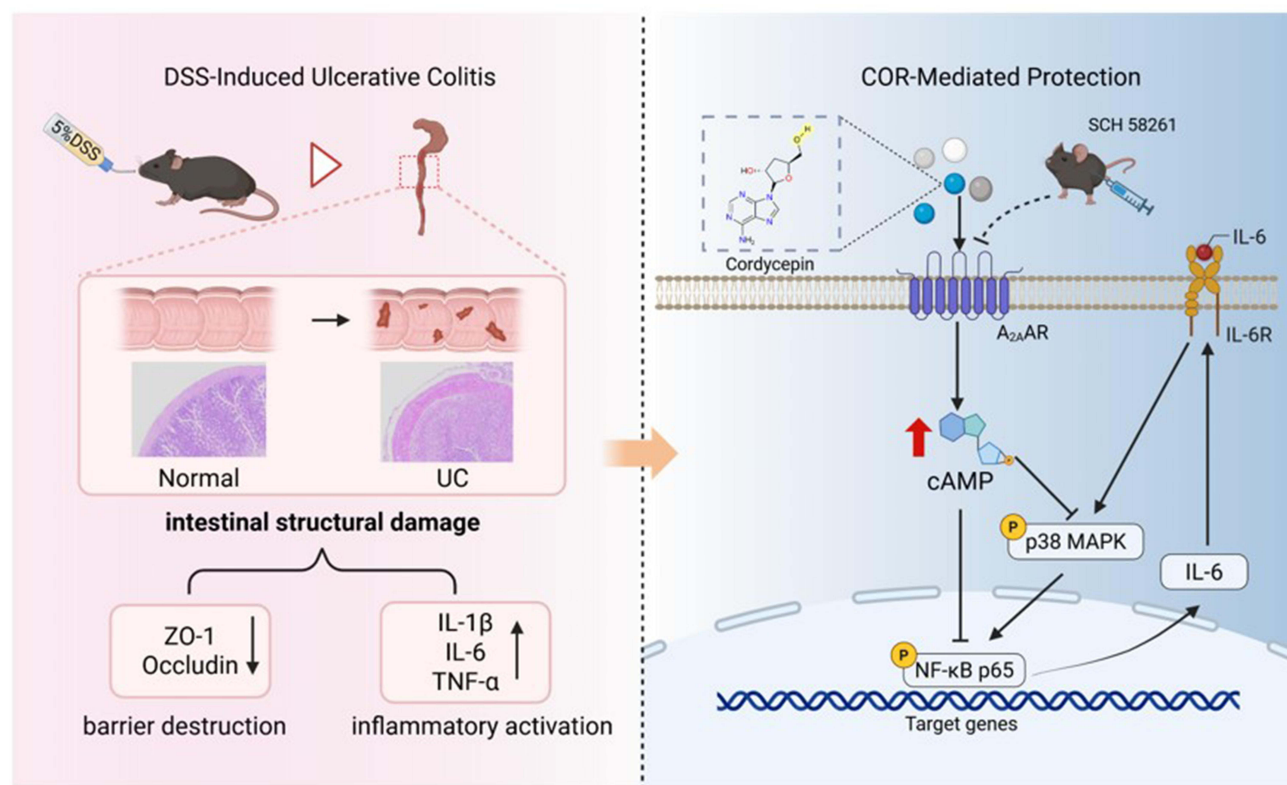


Figure 8 The ameliorative effect of cordycepin on DSS-induced colitis is attributed to its activation of $A_{2A}AR$, which inhibits IL-6/IL-6R-mediated phosphorylation activation of p38 MAPK and NF- κ B.

A_{2B}AR, and A₃AR, all of which belong to the G protein-coupled receptor superfamily.^{27,28} These receptors are widely distributed across various organs and tissues in the body and can be activated by the endogenous ligand adenosine, thereby regulating a range of critical physiological and pathological processes, including immune modulation, energy metabolism balance, cardiac function, and neuroprotection.^{27,28} The amino acid sequences of AR subtypes exhibit high homology, with considerable conservation in the ligand-binding pocket residues. Although adenosine is the endogenous ligand for AR, there are differences among receptor subtypes in terms of tissue distribution, expression levels, ligand binding affinity, and the downstream signaling pathways, which leading to distinct physiological effects.

During the process of cellular signal transduction, A₁AR and A₃AR preferentially couple with inhibitory G proteins (Gi), leading to suppressed adenylate cyclase (AC) activity and decreased intracellular cAMP levels.^{27,28} In contrast, A_{2A}AR couples with stimulatory Gs and, upon adenosine activation, can enhance AC activity, thereby increasing cAMP production and activating protein kinase A (PKA). Additionally, A_{2A}AR also exhibits coupling with Golf proteins, and its stimulatory effect on Golf proteins is similar to its activation effect on Gs proteins, both of which can amplify AC activity and cAMP generation. cAMP has long been recognized as an inducer of anti-inflammatory responses, and the cAMP-dependent pathway has been extensively utilized in pharmacological research for the treatment of inflammatory diseases.²⁶ A_{2B}AR, on the other hand, is capable of coupling with both Gs and Gq proteins, activating the PKA and phospholipase C γ signaling pathways respectively.^{27,28} By measuring cAMP levels in colonic epithelial cells, we observed that COR significantly upregulated cAMP levels. These results suggest that COR may activate A_{2A}AR and/or A_{2B}AR.

Based on the literature reports, we found that the role of A_{2A}AR in colitis is relatively consistent, and the activation of A_{2A}AR has the potential to improve colitis.^{13,29,30} For example, Pallio et al demonstrated that activating A_{2A}AR with the agonist polydeoxyribonucleotide significantly alleviated typical colitis symptoms in rats, such as weight loss, tissue damage, inflammatory cytokine levels, and myeloperoxidase activity, while A_{2A}AR antagonists could block this effect.²¹ Additionally, in mouse colitis model, inhibiting A_{2A}AR abolished the protective effect of the potent immunomodulator inosine on colonic injury.^{21,22} However, current research conclusions on A_{2B}AR in colitis are inconsistent, and its role in colitis remains unclear. Some studies suggest that the loss of A_{2B}AR function exacerbates the severity of colitis in mice,^{31,32} while others report the opposite conclusion: knockout or inhibition of A_{2B}AR reduces the severity and symptoms of DSS-induced colitis in mice.^{24,25} Thus, A_{2A}AR appears to be a more promising therapeutic target for UC. Furthermore, there are studies indicate that COR may exert neuroprotective effects, reduce body weight in obese mice, and promote tumor cell apoptosis by regulating different adenosine receptor subtypes (particularly A_{2A}AR and A₁AR).^{9,11,33} However, these studies have not yet fully elucidated the specific mechanisms underlying COR's regulation of adenosine receptors (whether it upregulates expression levels or activates the receptors). Additionally, no studies have reported whether activating AR in colonic epithelial cells has a protective effect or whether COR can regulate colonic epithelial cells and colitis by activating AR.

Based on existing literature reports and cAMP detection results, we preliminarily speculate that COR may exert its therapeutic effects by activating A_{2A}AR. We conducted preliminary verification using an A_{2A}AR inhibitor. The results showed that the A_{2A}AR inhibitor significantly suppressed the COR-induced elevation of cAMP levels and blocked COR's protective effect on DSS-damaged colonic epithelial cells. Furthermore, the A₁AR antagonist DPCPX neither inhibited the COR-induced increase in cAMP levels nor blocked COR's protection of DSS-damaged colonic epithelial cells, indirectly indicating that COR does not elevate cAMP levels by regulating A₁AR. Additionally, COR had no significant effect on the protein expression levels of A_{2A}AR and A₁AR. It is evident that the protective effect of A_{2A}AR activation on colonic epithelial cells aligns with the literature-reported outcomes of its ability to ameliorate colitis.^{13,20,21} These results preliminarily confirmed that COR protects colonic epithelial cells by activating A_{2A}AR rather than upregulating A_{2A}AR expression, and demonstrate the role of A_{2A}AR in colonic epithelial cells. However, we also observed that administering SCH alone to inhibit A_{2A}AR did not exacerbate DSS-induced colonic epithelial injury, suggesting that the degree of A_{2A}AR inhibition may not have a positive correlation with the extent of injury. The underlying reasons for this phenomenon warrant further investigation.

To verify whether COR directly interacts with A_{2A}AR, we conducted molecular docking and MD simulations between COR and A_{2A}AR. The results indicated that COR may form a stable binding with A_{2A}AR at the molecular

level through hydrogen bonds and hydrophobic interactions. Further *in vivo* validation experiments also confirmed that the effect of COR in the upregulation of serum cAMP levels in colitis mice was inhibited by SCH, thereby blocking its effects on alleviating colitis symptoms, reducing colonic inflammation, and improving intestinal barrier function. These demonstrated that COR is an A_{2A}AR agonist, which ameliorates DSS-induced colitis by activating A_{2A}AR.

To further elucidate the downstream protective mechanisms following COR-induced activation of A_{2A}AR, we conducted transcriptome sequencing analysis. The results revealed that the therapeutic effect of COR on colitis is closely associated with modulation of the IL-6 signaling pathway. Studies have demonstrated that the pleiotropic cytokine IL-6 drives intestinal inflammation and tissue remodeling in UC by regulating multiple pro-inflammatory signaling pathways, including JAK/STAT3, p38 MAPK, and NF-κB.^{34–36} Both basic research and clinical trials have shown that antibody therapies targeting IL-6R or IL-6 exhibit significant efficacy in treating colitis.^{24,37,38} Our further investigations demonstrated that COR-mediated activation of A_{2A}AR downregulates the expression of IL-6 and IL-6R in colonic tissues while suppressing the activation of key pro-inflammatory regulators NF-κB p65 and p38 MAPK.

Phosphorylation-induced activation of NF-κB p65 serves as a core mechanism driving intestinal inflammatory responses.^{39,40} P-p65 translocates into the nucleus and binds to the promoters of pro-inflammatory genes, directly upregulating the transcription of inflammatory mediators such as IL-6, TNF-α, and IL-1β. This process promotes neutrophil infiltration and M1 polarization of macrophages, leading to disruption of the intestinal mucosal barrier and tissue damage. Conversely, inhibition of p65 phosphorylation alleviates colitis symptoms. As a primary regulator of inflammatory responses within the MAPK family, phosphorylated activation of p38 MAPK drives inflammatory responses in colitis through multiple mechanisms, including phosphorylation of NF-κB p65 to facilitate its nuclear translocation.⁴¹ In addition, the anti-inflammatory substance cAMP can also inhibit the phosphorylation activation of p38 MAPK and NF-κB p65.²⁶ Thus, COR ameliorates DSS-induced colitis by activating A_{2A}AR to elevate cAMP levels, thereby blocking IL-6 / IL-6R to suppress p38 MAPK and NF-κB p65 activation.

In this study, we primarily focused on the protective effects of COR-activated A_{2A}AR on colonic epithelial cells, while not excluding its potential regulation of other cell types, such as T cells and macrophages.²² This is because COR has long been reported to possess immunomodulatory properties, and A_{2A}AR is also expressed in immune cells. Future research could employ single-cell technologies to identify all cell types regulated by COR and potentially evaluate their cellular contributions.

This study demonstrates the potential of cordycepin in alleviating colitis by activating the A_{2A} AR/cAMP axis and inhibiting the IL-6/p38 MAPK/NF-κB pathway, providing a theoretical basis for its clinical application in ulcerative colitis. However, future clinical translation still faces certain challenges, particularly concerning the pharmacokinetic properties of cordycepin. As reported in the literature, cordycepin is rapidly metabolized *in vivo* by adenosine deaminase, resulting in a short half-life and low bioavailability.⁴² Notably, co-administration with the adenosine deaminase inhibitor EHNA significantly prolongs the half-life of cordycepin and increases its plasma concentration (half-life extended to 23.3 min, AUC increased by approximately 92%). This suggests that improving its pharmacokinetic profile through formulation strategies (eg, sustained-release dosage forms, nano-encapsulation) or combination therapies may represent a feasible direction for promoting its clinical application. Future studies should focus on optimizing the dosing regimen to enhance *in vivo* stability and target-tissue distribution while ensuring safety.

Conclusion

This study confirms that COR can effectively protect colonic epithelial cells, inhibit intestinal inflammation, and improve intestinal barrier function, thereby significantly alleviating colitis induced by DSS. Mechanistic investigations revealed for the first time that the protective effect of COR against colitis primarily depends on the activation of A_{2A}AR to upregulate of cAMP levels. Further investigations demonstrated that COR activation of A_{2A}AR downregulated the expression of IL-6 and IL-6R in colon tissues, while inhibiting the phosphorylation activation of p38 MAPK and NF-κB p65, thereby exerting its protective effect against colitis. Together, these data suggest that COR acts as a potential A_{2A}AR agonist, providing data support for its potential application in the prevention and treatment of UC. Moreover, these results highlight the therapeutic potential of COR as a novel A_{2A}AR-targeted agent, which may represent a promising drug candidate for developing targeted therapies against ulcerative colitis.

Abbreviations

A_{2A}AR, adenosine receptor A_{2A}; AR, adenosine receptor; AB/PAS, alcian blue / periodic acid-Schiff; cAMP, cyclic adenosine monophosphate; COR, cordycepin; CRP, c-reactive protein; DAI, disease activity index; DAO, serum diamine oxidase; DSS, dextran sulfate sodium; H&E, hematoxylin and eosin; LDH, lactate dehydrogenase; MD, molecular dynamics; PI, propidium iodide; PME, particle mesh ewald; PPI, protein-protein interaction; Rg, radius of gyration. RMSF, root mean square fluctuation; SASP, sulfasalazine; SASA, solvent-accessible surface area; TUNEL, transferase-mediated dUTP Nick-end labeling; UC, ulcerative colitis; ZO-1, zonula Occludens-1.

Author Contributions

All authors made a significant contribution to the work reported, whether that is in the conception, study design, execution, acquisition of data, analysis and interpretation, or in all these areas; took part in drafting, revising or critically reviewing the article; gave final approval of the version to be published; have agreed on the journal to which the article has been submitted; and agree to be accountable for all aspects of the work.

Funding

This research was funded by the Joint Project on Regional High-Incidence Diseases Research of Guangxi Natural Science Foundation (No. 2024GXNSFBA010282), the National Natural Science Foundation of China (No.32500817), the Middle/Young aged Teachers' Research Ability Improvement Project of Guangxi Higher Education (No. 2024KY0136), the Youth Science Foundation of Guangxi Medical University (No. GXMUYSF202329), the Guangxi Zhuang Autonomous Region Administration of Traditional Chinese Medicine Self-funded Scientific Research Project (No.GXZYA20230269) and the Guangxi Medical University Student Innovation and Entrepreneurship Project (No. S202510598136).

Disclosure

The authors declare that there are no conflicts of interest in this work.

References

1. Ordás I, Eckmann L, Talamini M, Baumgart DC, Sandborn WJ. Ulcerative colitis. *Lancet*. 2012;380(9853):1606–1619. doi:10.1016/s0140-6736(12)60150-0
2. Park J, Cheon JH. Incidence and prevalence of inflammatory bowel disease across Asia. *Yonsei Med J*. 2021;62(2):99. doi:10.3349/ymj.2021.62.2.99
3. Segal JP, LeBlanc J-F, Hart AL. Ulcerative colitis: an update. *Clin Med*. 2021;21(2):135–139. doi:10.7861/clinmed.2021-0080
4. Tian X, Li Y, Shen Y, Li Q, Wang Q, Feng L. Apoptosis and inhibition of proliferation of cancer cells induced by cordycepin. *Oncol Lett*. 2015;10(2):595–599. doi:10.3892/ol.2015.3273
5. Yoon SY, Park SJ, Park YJ. The anticancer properties of cordycepin and their underlying mechanisms. *Int J Mol Sci*. 2018;19(10):3027. doi:10.3390/ijms19103027
6. Tan L, Song X, Ren Y, et al. Anti-inflammatory effects of cordycepin: a review. *Phytother Res*. 2021;35(3):1284–1297. doi:10.1002/ptr.6890
7. Liu Z, Wu S, Zhang W, et al. Cordycepin mitigates dextran sulfate sodium-induced colitis through improving gut microbiota composition and modulating Th1/Th2 and Th17/Treg balance. *Biomed Pharmacother*. 2024;180. 10.1016/j.biopha.2024.117394.
8. Chen J, Wang M, Zhang P, et al. Cordycepin alleviated metabolic inflammation in Western diet-fed mice by targeting intestinal barrier integrity and intestinal flora. *Pharmacol Res*. 2022;178. 10.1016/j.phrs.2022.106191.
9. Huang S-Y, Su Z-Y, Han -Y-Y, et al. Cordycepin improved the cognitive function through regulating adenosine A2A receptors in MPTP induced Parkinson's disease mice model. *Phytomedicine*. 2023;110. 10.1016/j.phymed.2023.154649.
10. Yoshikawa N, Yamada S, Takeuchi C, et al. Cordycepin (3'-deoxyadenosine) inhibits the growth of B16-BL6 mouse melanoma cells through the stimulation of adenosine A3 receptor followed by glycogen synthase kinase-3β activation and cyclin D1 suppression. *Naunyn-Schmiedeberg's Arch Pharmacol*. 2007;377(4–6):591–595. doi:10.1007/s00210-007-0218-y
11. Wang J, Gong Y, Tan H, et al. Cordycepin suppresses glutamatergic and GABAergic synaptic transmission through activation of A1 adenosine receptor in rat hippocampal CA1 pyramidal neurons. *Biomed Pharmacother*. 2022;145. doi:10.1016/j.biopha.2021.112446
12. An Y, Li Y, Wang X, et al. Cordycepin reduces weight through regulating gut microbiota in high-fat diet-induced obese rats. *Lipids Health Dis*. 2018;17(1). doi:10.1186/s12944-018-0910-6
13. Bahreyni A, Samani SS, Khazaei M, Ryzhikov M, Avan A, Hassanian SM. Therapeutic potentials of adenosine receptors agonists and antagonists in colitis; Current status and perspectives. *J Cell Physiol*. 2017;233(4):2733–2740. doi:10.1002/jcp.26073
14. Li D, Feng Y, Tian M, Ji J, Hu X, Chen F. Gut microbiota-derived inosine from dietary barley leaf supplementation attenuates colitis through PPARγ signaling activation. *Microbiome*. 2021;9(1). doi:10.1186/s40168-021-01028-7

15. Zhang S, Chen B, Wang B, et al. Effect of induction therapy with olamkicept vs placebo on clinical response in patients with active ulcerative colitis. *JAMA*. 2023;329(9). doi:10.1001/jama.2023.1084
16. Jo S, Kim T, Iyer VG, Im W. CHARMM-GUI: a web-based graphical user interface for CHARMM. *J Comput Chem*. 2008;29(11):1859–1865. doi:10.1002/jcc.20945
17. Mark P, Nilsson L. Structure and dynamics of liquid water with different long-range interaction truncation and temperature control methods in molecular dynamics simulations. *J Comput Chem*. 2002;23(13):1211–1219. doi:10.1002/jcc.10117
18. Wang Y, Li C, Li J, et al. Abelmoschus manihot polysaccharide fortifies intestinal mucus barrier to alleviate intestinal inflammation by modulating Akkermansia muciniphila abundance. *Acta Pharmaceutica Sinica B*. 2024;14(9):3901–3915. doi:10.1016/j.apsb.2024.06.002
19. Dieleman LA, Palmen MJ, Akol H, Bloemena E. Chronic experimental colitis induced by dextran sulphate sodium (DSS) is characterized by Th1 and Th2 cytokines. *Clin Exp Immunol*. 1998; 114:385–391.
20. Pallio G, Bitto A, Pizzino G, et al. Adenosine receptor stimulation by polydeoxyribonucleotide improves tissue repair and symptomology in experimental colitis. *Front Pharmacol*. 2016;7. doi:10.3389/fphar.2016.00273
21. Rahimian R, Fakhouri G, Daneshmand A, et al. Adenosine A2A receptors and uric acid mediate protective effects of inosine against TNBS-induced colitis in rats. *Eur J Pharmacol*. 2010;649(1–3):376–381. doi:10.1016/j.ejphar.2010.09.044
22. Mager L, Burkhard R, P N, et al. Microbiome-derived inosine modulates response to checkpoint inhibitor immunotherapy. *Science*. 2020;369(6510):1481–1489.
23. Grubišić V, Bali V, Fried DE, et al. Enteric glial adenosine 2B receptor signaling mediates persistent epithelial barrier dysfunction following acute DSS colitis. *Mucosal Immunol*. 2022;15(5):964–976. doi:10.1038/s41385-022-00550-7
24. Kolachala VL, Ruble BK, Vijay-Kumar M, et al. Blockade of adenosine A2B receptors ameliorates murine colitis. *Br J Pharmacol*. 2009;155(1):127–137. doi:10.1038/bjp.2008.227
25. Kolachala VL, Vijay-Kumar M, Dalmasso G, et al. A2B adenosine receptor gene deletion attenuates murine colitis. *Gastroenterology*. 2008;135(3):861–870. doi:10.1053/j.gastro.2008.05.049
26. Feng WG, Wang YB, Zhang JS, Wang XY, Li CL, Chang ZL. cAMP elevators inhibit LPS-induced IL-12 p40 expression by interfering with phosphorylation of p38 MAPK in Murine Peritoneal Macrophages. *Cell Res*. 2002;12(5–6):331–337. doi:10.1038/sj.cr.7290135
27. Borea PA, Gessi S, Merighi S, Vincenzi F, Varani K. Pharmacology of adenosine receptors: the state of the art. *Physiol Rev*. 2018;98(3):1591–1625. doi:10.1152/physrev.00049.2017
28. Kutryb-Zajac B, Kawecka A, Nasadiuk K, et al. Drugs targeting adenosine signaling pathways: a current view. *Biomed Pharmacother*. 2023;165. doi:10.1016/j.biopha.2023.115184
29. Tian T, Zhou Y, Feng X, et al. MicroRNA-16 is putatively involved in the NF- κ B pathway regulation in ulcerative colitis through adenosine A2a receptor (A2aAR) mRNA targeting. *Sci Rep*. 2016;6(1). doi:10.1038/srep30824
30. Zhang H, Li W. microRNA-15 activates NF- κ B pathway via down regulating expression of adenosine A2 receptor in ulcerative colitis. *Cell Physiol Biochem*. 2018;51(4):1932–1944. doi:10.1159/000495718
31. Frick J-S, MacManus CF, Scully M, Glover LE, Eltzschig HK, Colgan SP. Contribution of adenosine A2B receptors to inflammatory parameters of experimental colitis. *J Immunol*. 2009;182(8):4957–4964. doi:10.4049/jimmunol.0801324
32. Aherne CM, Saeedi B, Collins CB, et al. Epithelial-specific A2B adenosine receptor signaling protects the colonic epithelial barrier during acute colitis. *Mucosal Immunol*. 2015;8(6):1324–1338. doi:10.1038/mi.2015.22
33. Li Y, Li Y, Wang X, et al. Cordycepin modulates body weight by reducing prolactin via an adenosine A1 receptor. *Curr Pharm Des*. 2018;24(27):3240–3249. doi:10.2174/1381612824666180820144917
34. Zhao Y, Luan H, Jiang H, et al. Gegen Qinlian decoction relieved DSS-induced ulcerative colitis in mice by modulating Th17/Treg cell homeostasis via suppressing IL-6/JAK2/STAT3 signaling. *Phytomedicine*. 2021;84. 10.1016/j.phymed.2021.153519.
35. Yuan S-N, M-x W, Han J-L, et al. Improved colonic inflammation by nervonic acid via inhibition of NF- κ B signaling pathway of DSS-induced colitis mice. *Phytomedicine*. 2023;112. 10.1016/j.phymed.2023.154702.
36. Yang X-L, Guo T-K, Wang Y-H, et al. Ginsenoside Rd attenuates the inflammatory response via modulating p38 and JNK signaling pathways in rats with TNBS-induced relapsing colitis. *Int Immunopharmacol*. 2012;12(2):408–414. doi:10.1016/j.intimp.2011.12.014
37. Schreiber S, Aden K, Bernardes JP, et al. Therapeutic Interleukin-6 trans-signaling inhibition by olamkicept (sgp130Fc) in patients with active inflammatory bowel disease. *Gastroenterology*. 2021;160(7):2354–66.e11. doi:10.1053/j.gastro.2021.02.062
38. Neurath MF. Strategies for targeting cytokines in inflammatory bowel disease. *Nat Rev Immunol*. 2024;24(8):559–576. doi:10.1038/s41577-024-01008-6
39. Neurath MF, Becker C, Barbulescu K. Role of NF- κ B in immune and inflammatory responses in the gut. *Gut*. 1998;43(6):856–860. doi:10.1136/gut.43.6.856
40. Rogler G, Brand K, Vogl D, et al. Nuclear factor κ B is activated in macrophages and epithelial cells of inflamed intestinal mucosa. *Gastroenterology*. 1998;115(2):357–369. doi:10.1016/s0016-5085(98)70202-1
41. Zhang Y, Han J, Gao J, et al. Polysaccharide from Pyrus pashia Buch ameliorates DSS-induced colitis in mice via MAPK38/NF- κ B P65 and SCFAs/ERK/MSK signaling pathways. *Phytomedicine*. 2025;140. 10.1016/j.phymed.2025.156561.
42. Tsai Y-J, Lin L-C, Tsai T-H. Pharmacokinetics of adenosine and cordycepin, a bioactive constituent of cordyceps sinensis in rat. *J Agri Food Chem*. 2010;58(8):4638–4643. doi:10.1021/jf100269g

Drug Design, Development and Therapy

Publish your work in this journal

Drug Design, Development and Therapy is an international, peer-reviewed open-access journal that spans the spectrum of drug design and development through to clinical applications. Clinical outcomes, patient safety, and programs for the development and effective, safe, and sustained use of medicines are a feature of the journal, which has also been accepted for indexing on PubMed Central. The manuscript management system is completely online and includes a very quick and fair peer-review system, which is all easy to use. Visit <http://www.dovepress.com/testimonials.php> to read real quotes from published authors.

Submit your manuscript here: <https://www.dovepress.com/drug-design-development-and-therapy-journal>

Dovepress
Taylor & Francis Group